3-2002

The Quadruple System μ Orionis: Three-dimensional Orbit and Physical Parameters

Francis C. Fekel
Tennessee State University

Colin D. Scarfe
University of Victoria

David J. Barlow
University of Victoria

William I. Hartkopf
U.S. Naval Observatory

Brian D. Mason
U.S. Naval Observatory

See next page for additional authors

The Astronomical Journal, 123:1723–1740, 2002 March

THE QUADRUPLE SYSTEM μ ORIONIS: THREE-DIMENSIONAL ORBIT AND PHYSICAL PARAMETERS

Francis C. Fekel[1]
Center of Excellence in Information Systems, Tennessee State University, 330 10th Avenue North, Nashville, TN 37203-3401; fekel@evans.tsuniv.edu

C. D. Scarfe[2] and D. J. Barlow
Department of Physics and Astronomy, University of Victoria, Victoria, BC V8W 3P6, Canada; scarfe@uvic.ca, barlow@uvic.ca

William I. Hartkopf[1] and Brian D. Mason[1]
US Naval Observatory, 3450 Massachusetts Avenue, NW, Washington, DC 20392-5420; wih@usno.navy.mil, bdm@draco.usno.navy.mil

and

Harold A. McAlister[1]
Center for High Angular Resolution Astronomy, Georgia State University, Atlanta, GA 30303-3083; hal@chara.gsu.edu
Received 2001 November 20; accepted 2001 December 13

ABSTRACT

The star μ Orionis is a spectroscopic visual quadruple system in which each visual component is a short-period spectroscopic binary. The visual orbit has a period of 18.644 yr, a high eccentricity of 0.7426, and a high inclination of 96.°2. The visual primary consists of an Am star and probably a G or early K dwarf that orbit each other in a nearly circular orbit with a period of 4.4475858 days. The visual secondary consists of a pair of F5: V stars in a circular orbit with a period of 4.7835361 days. While the masses of the two stars are nearly identical and the magnitude difference between the pair is close to zero, the projected rotational velocities differ by almost a factor of 2. The orbit for the B subsystem is not coplanar with the visual orbit, while that for the A subsystem is probably not coplanar as well. The orbital parallax of $0''.02107 \pm 0''.00018$ is more accurate than that obtained from the *Hipparcos* observations and corresponds to a distance of 47.5 ± 0.4 pc. A comparison with evolutionary tracks indicates that the Am star is near the end of its main-sequence evolution.

Key words: binaries: close — stars: early-type — stars: individual (μ Orionis)

1. INTRODUCTION

The star μ Orionis (HR 2124 = HD 40932 = A2715 AB = ADS 4617, $\alpha = 06^h02^m23^s.0$, $\delta = +09°38'50''.1$ [J2000.0], $V = 4.13$) is a close quadruple system. Its primary, component Aa, is an Am star (Slettebak 1954; Abt & Morrell 1995).

Because it is a bright and relatively nearby system, μ Ori has been included in a variety of catalogs, and so it has numerous designations. One of the more interesting ones comes from van Bueren (1952), who assigned μ Ori number 169 in his list of possible members of the Hyades but determined that it is a nonmember. Later studies, such as those of Giclas, Burnham, & Thomas (1962) and Perryman et al. (1998), have come to the same conclusion.

Three components of μ Ori were found early in the 1900s, but it took nearly an additional three-quarters of a century for the inventory of stars to be completed. Frost's (1906) discovery of μ Ori as a single-lined spectroscopic binary, component Aa, was followed within a decade by Aitken's (1914) revelation that μ Ori is also a visual binary, components A and B. Using 124 radial velocities, Frost & Struve (1924) found Aa to have a period of 4.447 days and an essentially circular orbit. From its variable center-of-mass velocity, they determined rough elements of the visual binary system, including a period of 18 yr and an eccentricity of 0.6. Additional radial velocities by Frost, Barrett, & Struve (1929) near the time of the next periastron passage enabled Bourgeois (1929) to improve the long-period spectroscopic elements, the eccentricity being increased to 0.76. He also determined preliminary visual orbital elements.

Alden (1942) pointed out that although the magnitude difference of the visual pair is quite large, estimated to be greater than 2 mag by early visual observers, the B component appears to contain about 60% of the system's total mass, in apparent violation of the mass-luminosity relation. Computing a new visual orbit, as well as an astrometric orbit from photographic plates, he concluded that the reality of the large mass for component B was still open to question. As a result, he urged that additional spectroscopic observations be made during the next periastron passage. Such observations, obtained by Popper (1949), confirmed the high eccentricity of the visual orbit and the unexpectedly large mass ratio.

Our understanding of the system improved when Fekel (1980) solved the problem of the overmassive B component. He obtained red-wavelength spectrograms that showed B to be a double-lined spectroscopic binary consisting of two F-type stars, components Ba and Bb, having a period of 4.7838 days. Thus, the system is quadruple, containing a visual pair, each member of which consists of two components.

Labeyrie et al. (1974) resolved the visual components (AB) of μ Ori with speckle interferometry. This technique has been used by McAlister and collaborators (see Hartkopf, McAlister, & Mason 2001b) to obtain precise measurements of the visual pair. After the periastron passage of the long-period orbit at the beginning of 1985, Heintz

[1] Visiting Astronomer, Kitt Peak National Observatory, National Optical Astronomy Observatory (NOAO), operated by the Association of Universities for Research in Astronomy, Inc., under cooperative agreement with the National Science Foundation (NSF).

[2] Guest Worker, Dominion Astrophysical Observatory, Herzberg Institute of Astrophysics, National Research Council of Canada.

(1989) produced an improved orbit from observations that included some speckle measurements.

During the past four decades additional sets of spectroscopic observations of Aa, which cover only a portion of the long-period orbit, have been obtained at blue wavelengths. Scarfe (1967) presented 75 velocities from prism spectra taken by R. M. Petrie at the Dominion Astrophysical Observatory (DAO) up through 1964 February and revised the period of Aa to 4.447622 days. Abt, Sanwal, & Levy (1980) published 30 velocities from spectra obtained at Kitt Peak National Observatory (KPNO). Using seasonal means of their velocities, as well as additional velocities in the literature, and adopting the period, eccentricity, and longitude of periastron from Osvalds' (1964) orbit, they computed the other spectroscopic orbital elements for component A. As part of a study of metallic-line binaries, Abt & Levy (1985) published an additional 20 velocities from KPNO spectra.

With mostly his own unpublished observations, Fekel (1992) determined a preliminary long-period orbit for Aa using radial velocities alone. For elements in common, there was good agreement with the visual orbit of Heintz (1989). Söderhjelm's (1999) recent visual orbit, which resulted from a combination of *Hipparcos* astrometry and ground-based data, refined the visual elements still further.

Using 55 CORAVEL radial velocities of Aa obtained over a period of 14 yr plus constraints from additional spectroscopic and speckle observations, Debernardi et al. (2000) obtained orbital elements for Aa and AB. Their period for Aa is 4.44757 days and for AB, 6953 days or 19.04 yr.

High-resolution spectroscopic observations and speckle interferometry measurements have continued over the past decades at several observatories. Our extensive data sets and previously published observations of others enabled us to compute definitive spectroscopic and visual orbital elements for μ Ori. Using additional astrophysical data plus these elements, we have determined fundamental properties of the μ Ori system and its components.

2. RADIAL VELOCITY OBSERVATIONS AND REDUCTIONS

Between 1965 and 1999, photographic observations of μ Ori Aa have been obtained on Kodak IIa-O plates at the DAO, with the 1.2 m telescope and its coudé spectrograph. Initially, 16 plates were obtained between 1965 and 1969 at a reciprocal dispersion of 6.5 Å mm^{-1}. However, since the mosaic grating and image slicers (Richardson 1968) became available, observations have been made with them at 2.4 Å mm^{-1}. Between 1968 and 1999, 84 such plates were obtained, at least one in each season, except for 1971–1972 and 1978–1979, when the observer (C. D. S.) was away from Victoria for the whole observing season.

All the plates have been measured with the ARCTURUS measuring machine at DAO. The lines used are listed in Table 1, and a few whose rest wavelengths were adjusted to give zero mean velocity residual for all plates are specifically identified. Those lines gave highly consistent velocity offsets from the overall means and are believed to be unresolved blends. Some of the lines used at 2.4 Å mm^{-1} proved to be unsuitable for 6.5 Å mm^{-1}. Thus, several additional lines were measured on the latter plates, and those found to give consistent results were used to find the final velocities and are included in the table. Measurement of 12 plates of 68 Tau at 2.4 Å mm^{-1}, with the same lines as those used for μ Ori, gave a mean value of 38.9 $\pm$ 0.1 km s^{-1}, in excellent agreement with the result of Fekel (1999). This led us to anticipate that the DAO plates at that dispersion should show no significant difference in zero point from the KPNO data, an expectation that has been borne out in our orbital solutions. However, seven 6.5 Å mm^{-1} plates of 68 Tau, similarly treated, gave a mean velocity of 38.2 $\pm$ 0.2 km s^{-1}, and as a result, 0.7 km s^{-1} has been added to the raw velocities of μ Ori at that dispersion prior to our use of them for those solutions. The DAO observations of μ Ori are set out in Table 2.

TABLE 1
WAVELENGTHS OF STELLAR LINES MEASURED ON DAO PLATES

Wavelength (Å)	Identification	Wavelength (Å)	Identification
4215.554[a,b]	Sr II	4416.828.....	Fe II
4233.167.....	Fe II	4417.723.....	Ti II
4250.797[c]	Fe I	4443.812.....	Ti II
4290.226[c]	Ti II	4451.605[a,d]	Mn II
4294.092[a]	Ti II	4468.500.....	Ti II
4296.540[a]	Fe II	4481.227.....	Mg II
4300.048[c]	Fe I	4491.408[c]	Fe II
4303.156[a]	Fe II	4501.278.....	Ti II
4307.936[a]	Fe I	4508.289.....	Fe II
4325.787[a]	Fe I	4515.337.....	Fe II
4351.798.....	Fe II	4520.229.....	Fe II
4383.557.....	Fe I	4522.634.....	Fe II
4385.381.....	Fe II	4554.036[c]	Ba II
4395.040.....	Ti II	4558.659.....	Cr II
4395.846[d]	Ti II	4571.982[c]	Ti II
4404.761.....	Fe I	4583.816[a]	Fe II
4415.135.....	Fe I	4588.204[c]	Cr II

[a] Wavelength adjusted by residuals.
[b] The wavelength is 4215.539 Å for plates at 6.5 Å mm^{-1}.
[c] Used for plates at 6.5 Å mm^{-1} only.
[d] Used for plates at 2.4 Å mm^{-1} only.

Fifteen red-wavelength observations, obtained between 1977 and 1978 at McDonald Observatory, were published previously in Tables 1 and 3 of Fekel (1980). From 1979 to 1982, 19 additional spectrograms were acquired at McDonald Observatory with the 2.7 m telescope, coudé spectrograph, and a Reticon solid-state detector. Those observations, like the ones published previously by Fekel (1980), cover 100 Å centered at 6430 Å and have a resolution of either 0.22 or 0.33 Å.

From 1982 to 2001, 105 observations were collected at KPNO with the coudé feed telescope, coudé spectrograph, and various CCD detectors. Two spectra, having a central wavelength of 6410 Å, a wavelength range of 165 Å, and a resolution of 0.45 Å were taken with a Fairchild CCD during 1982 April. In 1983 January and April, six spectra, having a central wavelength of 6430 Å, a wavelength range of 65 Å, and a resolution of 0.30 Å were acquired with an RCA CCD. Over the past 17 yr, from 1983 September to 2001 April, the remaining 97 spectra were obtained with a TI CCD. Fifteen of those were centered at 4500 Å, while the rest were centered at 6430 Å. Both the blue- and red-wavelength spectrograms have a wavelength range of about 80 Å, a resolution of 0.21 Å, and a typical signal-to-noise ratio of 200–300.

Radial velocities were determined with the procedure of Fekel, Bopp, & Lacy (1978) or by cross-correlation with the

TABLE 2

DAO Radial Velocities of μ Ori Aa

HJD (−2,400,000)	Light-Time Correction (days)	ϕ_L	ϕ_S	V_{Aa} (km s^{-1})	$(O-C)_{Aa}$ (km s^{-1})
Plates at 6.5 Å mm^{-1}:					
39,057.033	−0.0103	0.968	0.882	83.6	0.8
39,141.814	−0.0047	0.980	0.943	92.8	0.9
39,187.760	−0.0013	0.987	0.273	61.9	0.8[a]
39,211.654	0.0006	0.991	0.645	47.0	−0.1
39,407.032	0.0112	0.019	0.571	23.1	−0.1
39,431.944	0.0118	0.023	0.172	61.6	−0.1
39,473.860	0.0123	0.029	0.597	21.0	−0.1
39,480.859	0.0124	0.030	0.170	59.2	0.1
39,553.704	0.0126	0.041	0.549	14.5	0.5
39,556.691	0.0126	0.041	0.220	48.0	0.5[b]
39,586.662	0.0125	0.046	0.959	70.4	0.5[b]
39,819.925	0.0100	0.080	0.407	13.3	−0.3
39,865.840	0.0093	0.087	0.730	34.9	0.8
40,160.990	0.0042	0.130	0.093	61.8	0.3
40,277.659	0.0020	0.147	0.326	23.8	0.4
40,289.662	0.0018	0.149	0.025	66.7	0.6
Plates at 2.4 Å mm^{-1}:					
40,104.002	0.0052	0.122	0.280	31.2	−0.4[b]
40,209.856	0.0033	0.137	0.081	62.5	−0.2
40,499.020	−0.0021	0.180	0.098	60.9	0.0
40,500.043	−0.0022	0.180	0.328	22.9	−0.2
40,542.839	−0.0030	0.186	0.950	65.3	0.2[b]
40,625.712	−0.0045	0.198	0.584	11.0	−0.4[b]
40,643.661	−0.0048	0.201	0.620	14.9	−0.4
40,647.644	−0.0049	0.202	0.515	7.4	−0.2
40,875.021	−0.0091	0.235	0.640	17.3	−0.9[c]
40,886.019	−0.0093	0.237	0.113	59.7	0.2
40,888.994	−0.0093	0.237	0.782	43.0	0.0
40,941.864	−0.0103	0.245	0.669	23.1	0.3
40,997.688	−0.0113	0.253	0.221	42.4	−0.1
41,621.073	−0.0215	0.345	0.386	16.1	0.2[b]
41,657.984	−0.0221	0.350	0.685	26.0	−0.2
41,942.017	−0.0261	0.392	0.548	10.4	0.2
42,114.623	−0.0284	0.417	0.358	20.1	−0.2[a]
42,306.010	−0.0308	0.445	0.390	16.4	0.1
42,319.033	−0.0310	0.447	0.318	27.0	0.2
42,327.052	−0.0311	0.448	0.121	60.4	0.2
42,392.866	−0.0319	0.458	0.919	65.2	0.2
42,513.643	−0.0332	0.476	0.075	65.4	−0.1
42,662.025	−0.0348	0.497	0.438	12.6	0.3
42,745.979	−0.0356	0.510	0.314	28.2	0.1
42,752.875	−0.0357	0.511	0.865	60.1	0.8[d]
42,801.820	−0.0361	0.518	0.870	59.9	−0.1
42,830.736	−0.0364	0.522	0.371	18.9	−0.7
42,843.700	−0.0365	0.524	0.286	32.4	−0.8[d]
43,041.009	−0.0382	0.553	0.650	23.2	0.5
43,110.950	−0.0387	0.563	0.375	20.2	0.7
43,215.617	−0.0394	0.579	0.909	64.6	−0.9[d]
43,488.875	−0.0410	0.619	0.349	24.2	0.2
43,501.830	−0.0411	0.621	0.262	39.0	0.1
43,550.741	−0.0413	0.628	0.259	39.2	−0.4
43,586.623	−0.0414	0.633	0.327	27.1	−0.6
44,149.047	−0.0423	0.716	0.783	49.4	0.4
44,197.878	−0.0423	0.723	0.762	45.3	0.0
44,320.637	−0.0420	0.741	0.363	24.5	0.3
44,580.954	−0.0408	0.779	0.893	67.0	−0.7
44,618.849	−0.0406	0.785	0.413	19.9	0.4
44,646.771	−0.0404	0.789	0.691	33.8	−0.2
45,021.786	−0.0364	0.844	0.009	76.5	0.2
45,048.624	−0.0360	0.848	0.043	75.3	−0.1
45,219.025	−0.0331	0.873	0.356	30.2	−0.1
45,349.766	−0.0303	0.892	0.751	49.7	−0.2

TABLE 2—*Continued*

HJD (−2,400,000)	Light-Time Correction (days)	ϕ_L	ϕ_S	V_{Aa} (km s^{-1})	$(O-C)_{Aa}$ (km s^{-1})
45,428.643	−0.0282	0.904	0.486	21.8	0.5
45,603.053	−0.0228	0.929	0.699	44.1	0.0
45,691.847	−0.0192	0.943	0.663	40.2	0.3
45,735.873	−0.0173	0.949	0.561	29.0	−0.1
45,933.009	−0.0059	0.978	0.883	85.3	−0.2
45,974.012	−0.0029	0.984	0.101	88.3	−0.2
46,036.922	0.0018	0.993	0.245	65.7	−0.3
46,099.682	0.0062	0.002	0.355	43.3	−0.1
46,161.648	0.0095	0.012	0.287	48.4	0.2
46,381.958	0.0126	0.044	0.821	54.4	0.0
46,465.823	0.0121	0.056	0.677	26.1	−0.6
46,520.673	0.0115	0.064	0.010	68.5	0.0
46,809.884	0.0071	0.107	0.037	66.0	0.0
46,886.708	0.0057	0.118	0.311	26.0	−0.2
47,043.016	0.0028	0.141	0.456	8.4	−0.2
47,089.960	0.0019	0.148	0.011	66.4	0.0
47,218.717	−0.0005	0.167	0.962	65.8	0.2
47,428.955	−0.0044	0.198	0.233	40.2	0.1
47,583.703	−0.0073	0.220	0.027	66.3	0.1
47,792.989	−0.0110	0.251	0.084	62.8	0.1
47,815.965	−0.0114	0.254	0.250	37.8	0.5
47,941.684	−0.0136	0.273	0.517	8.1	0.0
48,159.001	−0.0172	0.305	0.380	16.3	0.0
48,277.729	−0.0191	0.322	0.075	63.4	−0.6
48,514.992	−0.0228	0.357	0.423	12.2	0.1
49,036.806	−0.0299	0.434	0.749	38.7	0.0
49,230.028	−0.0322	0.462	0.194	49.4	0.2
49,265.038	−0.0326	0.467	0.066	66.3	0.2
49,304.009	−0.0330	0.473	0.828	53.2	−0.1
49,358.783	−0.0336	0.481	0.144	57.2	−0.3
49,383.722	−0.0339	0.485	0.751	39.8	0.2
49,615.017	−0.0362	0.519	0.756	41.1	0.2
49,739.846	−0.0373	0.537	0.823	53.1	−0.1
49,976.975	−0.0391	0.572	0.140	59.4	0.3
50,145.674	−0.0402	0.597	0.071	66.8	−0.6
50,510.723	−0.0418	0.650	0.149	59.1	0.1
50,714.044	−0.0423	0.680	0.864	61.8	0.1
51,084.019	−0.0421	0.734	0.050	71.3	0.0
51,444.051	−0.0404	0.787	0.999	74.1	−0.1

[a] Observed by A. H. Batten.
[b] Observed by J. M. Fletcher.
[c] Observed by J. B. Tatum. Exposed with the mosaic grating misaligned and given half-weight in the solution.
[d] 3 σ residual; velocity was not used in solution.

IRAF program FXCOR (Fitzpatrick 1993). Several spectra were measured with both techniques, and no systematic difference was found between the results. In the 6430 Å region, lines of Ba and Bb are visible (see Fig. 1 of Fekel 1980) but are so weak that only the best two or three lines, chosen by visual inspection, were used to obtain radial velocities of those components. For the red-wavelength spectra, the International Astronomical Union (IAU) radial velocity standards 10 Tau or β Vir were used. Their velocities of 27.9 and 4.4 km s^{-1}, respectively, were adopted from Scarfe, Batten, & Fletcher (1990). For the blue-wavelength spectra, the primary velocity standard was 68 Tau, although HR 2489 and HR 3383 were sometimes used. Velocities for those stars, adopted from Fekel (1999), are 39.0, 7.7, and 2.8 km s^{-1}, respectively.

All the McDonald Observatory and KPNO observations for component Aa are listed in Table 3, while those for Ba and Bb are given in Table 4. Some of the velocities differ slightly from those listed by Fekel (1980) because different radial velocities were adopted for two of the IAU standard stars.

3. VISUAL AND INTERFEROMETRIC OBSERVATIONS

Table 5 shows the visual and interferometric measurements of μ Ori = A2715 AB published through 2001 and tabulated in the database of the Washington Double Star Catalog (WDS; see Mason et al. 2001). Also listed is a single, previously unpublished, speckle interferometry measurement obtained at the KPNO 4 m telescope in 2001 January. Columns in Table 5 include the date of observation, expressed as fractional Besselian year, orbital phase, and the observed position angle θ in degrees and separation

TABLE 3

McDONALD AND KPNO RADIAL VELOCITIES OF μ ORI Aa

HJD (−2,440,000)	Light-Time Correction (days)	ϕ_L	ϕ_S	V_{Aa} (km s^{-1})	$(O-C)_{Aa}$ (km s^{-1})	Instrument Code[a]
43,447.996.....	−0.0408	0.613	0.158	56.1	−1.0	MR
43,449.997.....	−0.0408	0.613	0.608	18.8	0.9	MR
43,450.938.....	−0.0408	0.613	0.819	54.9[b]	1.4	MR
43,451.990.....	−0.0408	0.614	0.056	68.3	−0.4	MR
43,452.969.....	−0.0408	0.614	0.276	35.5	−0.8	MR
43,540.558.....	−0.0412	0.627	0.969	68.7	−1.6	MR
43,541.587.....	−0.0412	0.627	0.201	49.7	−0.4	MR
43,542.569.....	−0.0413	0.627	0.422	15.7	0.4	MR
43,620.596.....	−0.0416	0.638	0.965	72.2[b]	1.9	MR
43,621.599.....	−0.0416	0.638	0.191	52.5	0.5	MR
43,622.593.....	−0.0416	0.639	0.414	16.3	0.1	MR
43,740.975.....	−0.0420	0.656	0.032	69.0[b]	−1.6	MR
43,742.998.....	−0.0420	0.656	0.486	12.2[b]	−0.2	MR
43,744.004.....	−0.0420	0.656	0.713	32.9	−1.9	MR
43,744.999.....	−0.0420	0.657	0.936	66.9[b]	−2.1	MR
44,177.950.....	−0.0423	0.720	0.282	36.6[b]	−0.5	MR
44,178.896.....	−0.0423	0.720	0.494	12.9	−0.6	MR
44,179.933.....	−0.0423	0.720	0.727	39.0	0.3	MR
44,356.620.....	−0.0419	0.746	0.454	15.1	−0.3	MR
44,358.584.....	−0.0419	0.747	0.895	67.3	0.2	MR
44,360.589.....	−0.0419	0.747	0.346	27.4	0.5	MR
44,361.590.....	−0.0419	0.747	0.571	16.3	−0.6	MR
44,472.996.....	−0.0414	0.763	0.620	21.6	−0.7	MR
44,473.993.....	−0.0414	0.764	0.844	59.1	−1.4	MR
44,475.982.....	−0.0414	0.764	0.291	36.6	0.1	MR
44,531.004.....	−0.0411	0.772	0.662	29.0	0.3	MR
44,626.755.....	−0.0405	0.786	0.191	54.4	−0.8	MR
44,738.594.....	−0.0396	0.802	0.337	29.5	−0.5	MR
44,739.606.....	−0.0396	0.803	0.564	18.2	0.2	MR
44,833.990.....	−0.0387	0.817	0.786	52.8	0.6	MR
44,894.992.....	−0.0380	0.825	0.501	16.3	−0.2	MR
44,897.022.....	−0.0380	0.826	0.958	73.7	−0.9	MR
44,978.747.....	−0.0370	0.838	0.332	32.1	0.1	MR
45,076.686.....	−0.0356	0.852	0.353	28.6	−1.0	KF
45,078.647.....	−0.0355	0.852	0.794	50.8	−4.5[c]	KF
45,271.900.....	−0.0320	0.881	0.244	50.4	0.5	MR
45,356.750.....	−0.0301	0.893	0.322	36.0	−1.0	KR
45,356.804.....	−0.0301	0.893	0.334	35.1	0.0	KR
45,358.710.....	−0.0300	0.894	0.762	51.4	−0.7	KR
45,447.620.....	−0.0277	0.907	0.752	51.4	0.1	KR
45,449.627.....	−0.0277	0.907	0.204	60.8	1.5[c]	KR
45,451.650.....	−0.0276	0.907	0.658	35.0	0.2	KR
45,595.016.....	−0.0230	0.928	0.892	76.6	0.2	KT
45,599.031.....	−0.0229	0.929	0.795	66.4[b]	4.8	KT
45,717.731.....	−0.0181	0.946	0.482	26.7	−0.1	KT
45,719.641.....	−0.0180	0.947	0.912	80.3	−1.0	KT
45,721.895.....	−0.0179	0.947	0.418	29.9	−0.7	KT
45,784.677.....	−0.0149	0.956	0.534	28.6	−0.5	KT
45,812.655.....	−0.0134	0.960	0.824	72.1	−0.2	KT
45,813.630.....	−0.0133	0.960	0.043	85.6[b]	−1.8	KT
45,815.610.....	−0.0132	0.961	0.488	28.8	−0.9	KT
45,939.989.....	−0.0054	0.979	0.452	36.2	0.5	KT
46,076.831.....	0.0047	0.999	0.218	67.7[b]	−1.4	KT
46,079.947.....	0.0049	1.000	0.918	88.8	0.0	KT
46,130.626.....	0.0080	0.007	0.312	47.3	0.2	KT
46,133.652.....	0.0082	0.007	0.992	88.5[b]	1.0	KT
46,340.988.....	0.0126	0.038	0.609	19.7	−0.2	KT
46,374.968.....	0.0126	0.043	0.249	41.8	−0.1	KT
46,388.866.....	0.0126	0.045	0.374	20.3	−0.5	KT
46,389.887.....	0.0126	0.045	0.604	18.3	0.5	KT
46,530.624.....	0.0114	0.066	0.247	38.9	−0.5	KT
46,532.671.....	0.0113	0.066	0.708	30.6	−0.5	KT
46,722.027.....	0.0086	0.094	0.283	30.9	−0.6	KT

TABLE 3—*Continued*

HJD (−2,440,000)	Light-Time Correction (days)	ϕ_L	ϕ_S	V_{Aa} (km s^{-1})	$(O-C)_{Aa}$ (km s^{-1})	Instrument Code[a]
46,766.805.....	0.0078	0.100	0.351	19.8	−0.2	KT
46,814.840.....	0.0070	0.107	0.152	54.9	0.7	KT
46,867.647.....	0.0060	0.115	0.025	66.5	0.2	KT
46,868.601.....	0.0060	0.115	0.240	38.9[b]	−0.1	KT
47,151.917.....	0.0008	0.157	0.942	65.3	0.7	KT
47,152.847.....	0.0008	0.157	0.151	54.2	0.2	KT
47,245.619.....	−0.0010	0.171	0.010	67.0	0.6	KT
47,248.683.....	−0.0010	0.171	0.699	28.0	0.4	KT
47,455.960.....	−0.0049	0.202	0.305	27.1	0.0	KT
47,458.045.....	−0.0050	0.202	0.773	40.7	−0.6	KT
47,459.008.....	−0.0050	0.202	0.990	66.6	0.1	KT
47,556.808.....	−0.0068	0.216	0.980	65.5	−0.9	KT
47,623.635.....	−0.0080	0.226	0.006	66.8	0.2	KT
47,626.596.....	−0.0080	0.227	0.671	23.2[b]	0.2	KT
47,809.987.....	−0.0113	0.254	0.906	61.7	−0.2	KT
47,813.020.....	−0.0114	0.254	0.588	12.7[b]	0.7	KT
47,815.000.....	−0.0114	0.254	0.033	66.1	0.0	KT
47,917.725.....	−0.0132	0.269	0.130	57.8	0.4	KT
48,005.655.....	−0.0147	0.282	0.901	61.3	−0.3	KT
48,006.636.....	−0.0147	0.282	0.121	59.0	0.3	KT
48,345.681.....	−0.0202	0.332	0.354	20.7	0.6	KT
48,348.659.....	−0.0203	0.333	0.023	67.6	0.5	KT
48,508.997.....	−0.0227	0.356	0.075	65.2	0.9	KT
48,606.756.....	−0.0241	0.371	0.055	65.9	0.0	KT
48,607.838[d]	−0.0241	0.371	0.298	29.3	−0.1	KT
48,912.981.....	−0.0283	0.416	0.908	63.8	0.3	KT
48,916.900[d]	−0.0284	0.416	0.789	45.8	−0.1	KT
49,101.617.....	−0.0307	0.443	0.322	26.4	0.3	KT
49,104.651.....	−0.0307	0.444	0.004	69.0	0.5	KT
49,105.632[d]	−0.0307	0.444	0.224	43.2	−0.4	KT
49,246.029.....	−0.0324	0.465	0.792	46.8	−0.1	KT
49,246.998[d]	−0.0324	0.465	0.010	68.0	−0.6	KT
49,248.017.....	−0.0324	0.465	0.239	41.4	0.2	KT
49,251.933[d]	−0.0324	0.465	0.119	59.8	−0.8	KT
49,302.922.....	−0.0330	0.473	0.584	14.1	0.5	KT
49,307.959.....	−0.0331	0.474	0.716	33.3	0.3	KT
49,458.656.....	−0.0346	0.496	0.600	15.6	0.1	KT
49,460.641.....	−0.0347	0.496	0.046	67.4	−0.4	KT
49,460.679.....	−0.0347	0.496	0.055	67.4	0.1	KT
49,462.598[d]	−0.0347	0.496	0.486	10.0	−0.2	KT
49,620.007.....	−0.0362	0.519	0.878	61.4	0.2	KT
49,620.998.....	−0.0362	0.520	0.101	63.2	−0.2	KT
49,677.932[d]	−0.0367	0.528	0.902	63.4	−0.7	KT
49,834.611.....	−0.0380	0.551	0.131	59.1[b]	−1.1	KT
49,835.631.....	−0.0381	0.551	0.360	22.4	0.9	KT
49,836.618[d]	−0.0381	0.551	0.582	13.6	−0.8	KT
49,969.993.....	−0.0391	0.571	0.570	13.7	0.0	KT
50,199.608.....	−0.0405	0.605	0.197	50.6	0.2	KT
50,201.628.....	−0.0405	0.605	0.652	24.6	0.9	KT
50,203.616[d]	−0.0405	0.605	0.099	64.5	−0.3	KT
50,361.977.....	−0.0413	0.628	0.705	33.2	0.3	KT
50,364.037.....	−0.0413	0.629	0.168	54.9	−0.8	KT
50,366.901[d]	−0.0413	0.629	0.812	52.1	−0.4	KT
50,399.958.....	−0.0415	0.634	0.245	42.5	0.2	KT
50,404.791[d]	−0.0415	0.635	0.331	27.1	0.1	KT
50,577.618.....	−0.0420	0.660	0.190	52.9	0.4	KT
50,721.028.....	−0.0423	0.681	0.434	14.6	−0.6	KT
50,753.918.....	−0.0423	0.686	0.830	56.8	0.3	KT
50,758.947.....	−0.0424	0.687	0.960	70.4	−0.6	KT
50,830.805.....	−0.0424	0.697	0.117	64.3	0.0	KT
50,833.682[d]	−0.0424	0.698	0.764	44.9	−0.1	KT
50,833.787.....	−0.0424	0.698	0.787	49.2	−0.2	KT
50,926.620.....	−0.0424	0.711	0.660	27.2	0.4	KT
50,928.609.....	−0.0424	0.712	0.107	65.9	0.2	KT

TABLE 3—*Continued*

HJD (−2,440,000)	Light-Time Correction (days)	ϕ_L	ϕ_S	V_{Aa} (km s^{-1})	$(O-C)_{Aa}$ (km s^{-1})	Instrument Code[a]
50,931.617[d]	−0.0424	0.712	0.784	48.5	−0.5	KT
51,088.968[d]	−0.0421	0.735	0.162	57.8	−0.8	KT
51,092.040.....	−0.0421	0.736	0.853	61.1	−0.1	KT
51,093.963.....	−0.0421	0.736	0.286	36.9	0.1	KT
51,304.610.....	−0.0413	0.767	0.647	26.7	0.5	KT
51,306.613.....	−0.0413	0.767	0.098	68.3	0.2	KT
51,471.951.....	−0.0402	0.791	0.272	40.7	0.0	KT
51,473.959.....	−0.0402	0.792	0.724	39.7	−0.2	KT
51,658.643[d]	−0.0385	0.819	0.248	45.6	−0.5	KT
51,804.010.....	−0.0368	0.840	0.932	73.4	−0.2	KT
52,014.638.....	−0.0333	0.871	0.289	41.4	0.3	KT
52,016.627.....	−0.0333	0.871	0.736	46.3	0.6	KT

[a] Instrument code: (MR) McDonald Reticon, (KF) KPNO Fairchild CCD, (KR) KPNO RCA CCD, and (KT) KPNO Texas Instruments CCD.
[b] Component was blended; velocity was not used in orbital solution.
[c] 3 σ residual; velocity was not used in orbital solution.
[d] Observation at 4500 Å.

TABLE 4

McDonald and KPNO Radial Velocities of μ Ori Ba and Bb

HJD (−2,440,000)	Light Time Correction (days)	ϕ_L	ϕ_S	V_{Ba} (km s^{-1})	$(O-C)_{Ba}$ (km s^{-1})	V_{Bb} (km s^{-1})	$(O-C)_{Bb}$ (km s^{-1})
43,447.996.....	0.045	0.613	0.107	108.0	−0.1	−19.3	1.9
43,449.997.....	0.045	0.613	0.526	−36.2	0.3	128.8	1.9
43,450.938.....	0.045	0.613	0.722	31.8	1.7	[a]	...
43,451.990.....	0.045	0.614	0.942	119.3	−1.4	−34.0	0.1
43,452.969.....	0.045	0.614	0.147	94.2	0.7	−6.0	0.3
43,540.558.....	0.046	0.627	0.457	−36.9	−2.0	123.3	−1.4
43,541.587.....	0.046	0.627	0.672	5.6	−0.1	82.8	−0.4
43,542.569.....	0.046	0.627	0.878	103.6	0.8	−19.7	−3.5
43,620.596.....	0.046	0.638	0.189	[a]	...	14.8	2.2
43,621.599.....	0.046	0.638	0.399	−21.9	0.2	112.9	1.7
43,622.593.....	0.046	0.639	0.607	−20.1	0.2	109.3	−0.1
43,740.975.....	0.046	0.656	0.354	−6.7	−0.3	[a]	...
43,742.998.....	0.046	0.656	0.777	56.8	−0.6	[a]	...
43,744.004.....	0.046	0.656	0.988	122.4	−2.6	−37.2	2.8
43,744.999.....	0.046	0.657	0.196	[a]	...	13.6	−1.8
44,178.896.....	0.047	0.720	0.902	108.9	0.1	−26.0	0.3
44,179.933.....	0.047	0.720	0.119	101.5	−0.7	−18.2	1.2
44,356.620.....	0.046	0.746	0.055	116.8	−1.5	−37.1	0.2
44,358.584.....	0.046	0.747	0.466	−37.1	1.4	123.5	0.3
44,360.589.....	0.046	0.747	0.885	103.3	0.6	−18.5	2.9
44,361.590.....	0.046	0.747	0.094	108.9	−0.3	−28.6	−0.5
44,472.996.....	0.046	0.763	0.384	−19.4	0.6	106.0	2.7
44,475.982.....	0.046	0.764	0.008	121.8	−0.8	−42.9	−0.2
44,531.004.....	0.046	0.772	0.510	−41.7	−0.8	118.9	−5.3[b]
44,626.755.....	0.045	0.786	0.527	−42.5	−2.1	122.7	0.0
44,738.594.....	0.044	0.802	0.908	108.8	0.8	−31.7	−1.3
44,739.606.....	0.044	0.803	0.119	102.4	2.9	−20.7	1.0
44,833.990.....	0.043	0.816	0.850	87.8	0.5	−9.0	1.3
44,894.992.....	0.042	0.825	0.603	−24.4	2.2	105.4	−0.1
44,978.747.....	0.041	0.838	0.112	100.2	−0.2	−27.0	−1.4
45,076.686.....	0.039	0.852	0.587	−35.6	−3.0	106.4	−2.5
45,078.647.....	0.039	0.852	0.997	114.3	−4.8	−51.2	−4.8
45,271.900.....	0.035	0.881	0.397	−28.5	1.3	102.0	−0.4
45,356.750.....	0.033	0.893	0.136	89.6	1.2	−24.5	−3.9
45,358.710.....	0.033	0.894	0.545	−42.0	2.0	110.1	−4.8
45,447.620.....	0.031	0.907	0.133	86.6	−1.7	−20.0	3.1
45,449.627.....	0.031	0.907	0.552	−41.8	2.4	117.1	4.6
45,451.650.....	0.031	0.907	0.975	116.7	2.7	−45.8	3.7

TABLE 4—*Continued*

HJD (−2,440,000)	Light Time Correction (days)	ϕ_L	ϕ_S	V_{Ba} (km s^{-1})	$(O-C)_{Ba}$ (km s^{-1})	V_{Bb} (km s^{-1})	$(O-C)_{Bb}$ (km s^{-1})
45,595.016.....	0.026	0.928	0.947	108.2	0.3	−48.1	0.4
45,599.031.....	0.025	0.929	0.786	[a]	...	10.9	−0.8
45,717.731.....	0.020	0.946	0.602	−40.1	−2.0	95.4	0.6
45,719.641.....	0.020	0.947	0.001	108.9	−0.4	−56.0	0.2
45,721.895.....	0.020	0.947	0.472	−53.1	0.0	110.5	0.6
45,784.677.....	0.016	0.956	0.597	−41.0	0.5	95.0	1.1
45,812.655.....	0.015	0.960	0.447	−53.6	−0.8	103.4	0.0
45,813.630.....	0.015	0.960	0.650	−24.3	−0.7	[a]	...
45,815.610.....	0.015	0.961	0.064	100.0	0.6	−51.0	1.7
45,939.989.....	0.006	0.979	0.068	96.8	3.3[b]	−59.9	−2.6
46,076.831.....	−0.005	0.999	0.677	−16.0	0.7	[a]	...
46,079.947.....	−0.005	0.999	0.328	−19.2	−0.4	57.8	−1.6
46,130.626.....	−0.009	0.007	0.923	97.7	0.1	−48.6	0.6
46,133.652.....	−0.009	0.007	0.556	−51.0	0.3	[a]	...
46,340.988.....	−0.014	0.038	0.901	109.0	0.4	−24.1	1.7
46,374.968.....	−0.014	0.043	0.004	124.6	−0.5	−38.5	1.8
46,388.866.....	−0.014	0.045	0.910	112.5	−0.3	−27.3	−0.5
46,389.887.....	−0.014	0.045	0.123	102.1	−0.2	−17.0	−0.9
46,530.624.....	−0.013	0.066	0.544	−32.1	0.1	127.0	−0.1
46,532.671.....	−0.012	0.066	0.972	125.6	−1.5	−35.4	0.5
46,722.027.....	−0.009	0.094	0.556	−29.1	−0.4	125.8	−0.8
46,766.805.....	−0.009	0.100	0.917	118.8	−0.3	−24.5	−0.1
46,814.840.....	−0.008	0.107	0.958	128.0	0.6	−33.2	−0.7
46,867.647.....	−0.007	0.115	0.998	130.8	0.5	−36.0	−0.8
47,151.917.....	−0.001	0.157	0.423	−23.4	0.2	124.5	1.6
47,152.847.....	−0.001	0.157	0.618	−13.0	−1.3	109.7	−1.0
47,245.619.....	0.001	0.171	0.011	130.9	0.5	−34.5	0.3
47,248.683.....	0.001	0.171	0.652	−1.1	−2.5	99.8	2.5
47,455.960.....	0.005	0.202	0.982	129.5	−0.4	−36.4	−1.9
47,458.045.....	0.005	0.202	0.418	−23.3	−0.8	121.6	0.1
47,459.008.....	0.005	0.202	0.619	−9.6	1.6	110.2	0.2
47,556.808.....	0.007	0.216	0.064	123.6	−0.3	−30.3	−1.8
47,623.635.....	0.009	0.226	0.034	128.3	−0.2	−32.1	1.2
47,626.596.....	0.009	0.227	0.653	[a]	...	95.5	−1.0
47,809.987.....	0.013	0.253	0.990	130.1	0.1	−35.6	−0.4
47,813.020.....	0.013	0.254	0.624	[a]	...	107.0	−0.9
47,815.000.....	0.013	0.254	0.038	126.2	−1.6	−34.1	−1.1
47,917.725.....	0.015	0.269	0.512	−32.0	1.3	131.3	−0.4
48,005.655.....	0.016	0.282	0.894	111.7	−0.7	−17.1	0.5
48,006.636.....	0.016	0.282	0.099	114.2	−0.4	−19.3	0.7
48,345.681.....	0.022	0.332	0.975	130.1	1.6	−34.9	0.1
48,348.659.....	0.022	0.333	0.598	−18.3	0.9	116.8	0.6
48,508.997.....	0.025	0.356	0.116	109.7	1.2	−13.9	1.2
48,606.756.....	0.027	0.370	0.552	−31.5	−1.4	128.5	1.9
48,912.981.....	0.031	0.415	0.567	−27.8	−0.1	124.3	1.1
49,101.617.....	0.034	0.443	0.001	129.1	0.8	−37.2	0.0
49,104.651.....	0.034	0.444	0.636	−6.9	0.4	102.3	0.6
49,246.029.....	0.036	0.464	0.190	75.4	−0.8	17.6	2.0
49,248.017.....	0.036	0.465	0.606	−18.2	−0.2	112.6	0.5
49,302.922.....	0.037	0.473	0.084	117.7	0.8	−26.1	0.1
49,307.959.....	0.037	0.473	0.137	99.5	−0.1	−9.6	−1.1
49,458.656.....	0.038	0.496	0.640	[a]	...	99.3	−0.1
49,460.641.....	0.038	0.496	0.055	121.5	−1.4	−31.4	1.6
49,460.679.....	0.038	0.496	0.063	121.0	−0.4	−31.8	−0.3
49,620.007.....	0.040	0.519	0.370	−10.2	0.1	103.2	0.4
49,620.998.....	0.040	0.519	0.577	−26.8	0.0	120.8	1.1
49,835.630.....	0.042	0.551	0.445	−32.0	−0.1	123.9	−0.1
49,969.993.....	0.043	0.571	0.534	−36.2	−1.1	125.8	−0.9
50,199.608.....	0.045	0.604	0.535	−35.5	0.0	125.5	−0.6
50,201.628.....	0.045	0.605	0.957	121.7	−1.4	−38.8	−2.5
50,361.977.....	0.046	0.628	0.478	−37.5	−0.5	125.2	−1.7
50,364.037.....	0.046	0.629	0.908	112.5	0.0	−25.0	1.3
50,399.958.....	0.046	0.634	0.418	−27.1	0.1	115.7	−0.9
50,577.618.....	0.047	0.660	0.557	−33.2	0.0	120.2	−1.5

TABLE 4—*Continued*

HJD (−2,440,000)	Light Time Correction (days)	ϕ_L	ϕ_S	V_{Ba} (km s^{-1})	$(O-C)_{Ba}$ (km s^{-1})	V_{Bb} (km s^{-1})	$(O-C)_{Bb}$ (km s^{-1})
50,721.028.....	0.047	0.681	0.537	−37.7	−1.1	124.4	0.0
50,753.918.....	0.047	0.686	0.413	−27.2	−0.2	114.2	−0.2
50,758.947.....	0.047	0.687	0.464	−36.0	0.9	123.3	−1.2
50,830.805.....	0.047	0.697	0.486	−39.5	−0.6	125.1	−0.9
50,833.787.....	0.047	0.698	0.109	105.0	−0.8	−22.8	−0.7
50,926.620.....	0.047	0.711	0.516	−39.5	−0.4	125.6	0.0
50,928.609.....	0.047	0.711	0.932	117.2	0.5	−35.0	−1.1
51,092.040.....	0.047	0.735	0.097	108.6	0.0	−25.2	1.6
51,093.963.....	0.047	0.736	0.499	−39.6	0.5	125.7	0.3
51,304.610.....	0.046	0.767	0.535	−38.6	0.3	121.9	−0.6
51,306.613.....	0.046	0.767	0.954	118.8	−0.4	−41.0	−1.5
51,471.951.....	0.045	0.791	0.518	−42.1	−0.9	123.3	0.1
51,473.959.....	0.045	0.792	0.938	115.2	−0.5	−36.6	0.9
51,804.010.....	0.041	0.840	0.936	113.2	−0.1	−39.8	−0.7
52,014.638.....	0.037	0.871	0.969	116.2	−0.2	−45.6	0.3
52,016.627.....	0.037	0.871	0.385	−25.0	0.1	100.2	1.3

[a] Component was blended with Aa.
[b] 3 σ residual; velocity was not used in orbital solution.

TABLE 5
VISUAL AND INTERFEROMETRIC MEASUREMENTS

Besselian Year	Phase	θ (deg)	$(O-C)_\theta$ (deg)	ρ (arcsec)	$(O-C)_\rho$ (arcsec)	Weight	Telescope Size (m)	Observing Technique[a]
1914.74	0.228	32.0	8.4	0.36	0.00	0.8[b]	0.9	M
1919.966.....	0.509	25.8	5.7	0.38	0.00	0.3	1.0	M
1924.237.....	0.738	18.0	2.8	0.20	−0.02	0.3	1.0	M
1926.94	0.883	350.0	1.3	0.13	0.08	0.1	0.7	M
1927.04	0.888	348.0	4.1	0.12	0.08	0.1	0.7	M
1931.93	0.150	23.9	−1.1	0.27	−0.02	0.7	0.7	M
1933.81	0.251	23.6	0.3	0.41	0.04	0.1	0.7	M
1935.00	0.315	21.0	−1.5	0.32	−0.08	0.4	0.9	M
1935.19	0.325	20.2	−2.1	0.43	0.03	0.5	0.9	M
1935.19	0.325	24.8	2.5	0.42	0.02	0.5	0.3	M
1935.84	0.360	23.0	1.1	0.39	−0.01	0.4	0.4	M
1935.86	0.361	24.4	2.5	0.28	−0.12	0.5[b]	0.4	M
1936.04	0.371	20.6	−1.2	0.32	−0.08	0.6	0.7	M
1936.83	0.413	25.1	3.8	0.41	0.01	0.3	0.4	M
1937.12	0.429	24.2	3.1	0.39	−0.01	0.9	0.7	M
1937.70	0.460	21.7	0.9	0.35	−0.04	0.4	0.3	M
1937.78	0.464	24.2	3.5	0.39	0.00	0.4	0.6	M
1938.10	0.481	23.1	2.6	0.33	−0.06	0.8	0.7	M
1939.80	0.573	23.8	4.6	0.30	−0.05	0.5	0.6	M
1939.92	0.579	64.5	45.4	0.19	−0.15	0.1[b]	0.5	E
1940.55	0.613	17.8	−0.7	0.28	−0.04	0.3	1.0	M
1941.07	0.641	16.6	−1.4	0.27	−0.03	0.4	0.7	M
1942.06	0.694	10.7	−6.0	0.25	−0.01	0.2	1.0	M
1943.81	0.788	7.6	−4.9	0.16	0.00	0.3	2.1	M
1950.75	0.160	21.8	−3.0	0.26	−0.04	0.2	1.0	M
1951.05	0.176	20.7	−3.8	0.24	−0.08	0.3	2.1	M
1951.58	0.205	29.8	5.8	0.34	0.00	0.6	0.7	M
1953.02	0.282	22.8	−0.1	0.30	−0.08	0.7	2.1	M
1953.20	0.292	22.1	−0.6	0.42	0.03	1.1	0.4	M
1953.22	0.293	24.0	1.3	0.39	0.00	0.2	0.5	M
1954.18	0.344	20.9	−1.2	0.44	0.04	0.2	0.5	M
1955.78	0.430	24.6	3.5	0.34	−0.06	0.7	2.1	M
1955.83	0.433	21.9	0.8	0.37	−0.03	0.8	0.4	M
1956.11	0.448	20.4	−0.5	0.38	−0.01	0.1	0.3	M
1956.16	0.450	19.0	−1.9	0.34	−0.05	0.3	0.6	M
1957.94	0.546	23.0	3.0	0.29	−0.07	0.2	0.3	M
1958.09	0.554	18.7	−0.8	0.29	−0.07	0.1	0.4	M

TABLE 5—*Continued*

Besselian Year	Phase	θ (deg)	$(O-C)_\theta$ (deg)	ρ (arcsec)	$(O-C)_\rho$ (arcsec)	Weight	Telescope Size (m)	Observing Technique[a]
1958.15	0.557	27.0	7.5	0.31	−0.04	0.5	1.0	M
1960.00	0.656	19.2	1.6	0.29	0.00	0.8	0.9	M
1960.89	0.704	17.3	0.9	0.24	−0.01	0.7	0.9	M
1961.89	0.758	8.4	−5.9	0.15	−0.04	0.4	0.9	M
1962.87	0.810	9.4	−1.2	0.13	−0.01	0.3	0.9	M
1969.120.....	0.146	26.1	1.0	0.26	−0.02	0.6	0.7	M
1971.22	0.258	20.0	−3.2	0.37	−0.01	0.7	0.4	M
1971.243.....	0.259	20.5	−2.7	0.30	−0.08	0.1	0.5	M
1972.960.....	0.352	338.0	−44.0	0.290	−0.112	5.0[b]	5.0	S
1973.200.....	0.364	337.0	−45.0	0.274	−0.129	5.0[b]	5.0	S
1975.94	0.511	20.0	−0.1	0.33	−0.05	0.4	0.6	M
1975.953.....	0.512	17.7	−2.4	0.374	−0.001	0.3	2.5	S
1975.9566.....	0.512	21.0	0.9	0.376	0.001	28.2	3.8	S
1976.8603.....	0.561	20.0	0.6	0.360	0.008	28.1	3.8	S
1976.9231.....	0.564	19.6	0.3	0.359	0.009	28.1	3.8	S
1977.11	0.574	23.8	4.6	0.25	−0.09	0.2	0.6	M
1977.1798.....	0.578	22.1	3.0	0.349	0.006	11.4[b]	2.1	S
1977.8818.....	0.616	18.5	0.0	0.311	−0.008	0.2	2.5	S
1977.9143.....	0.617	15.4	−3.0	0.316	−0.002	9.2[b]	2.1	S
1978.8730.....	0.669	17.0	−0.3	0.384	0.105	0.1	3.9	S
1979.1922.....	0.686	14.4	−2.5	0.276	0.012	7.1[b]	2.1	S
1980.7264.....	0.768	13.7	−0.1	0.184	0.000	11.2	3.8	S
1980.7292.....	0.768	13.9	0.1	0.184	0.000	11.2	3.8	S
1980.7773.....	0.771	13.0	−0.6	0.184	0.003	8.1	6.0	S
1980.939.....	0.780	12.2	−0.9	0.153	−0.018	0.4	1.5	S
1984.0632.....	0.947	283.4	62.7	0.170	0.115	9.5[b]	3.8	S
1985.8544.....	0.043	31.8	0.0	0.089	0.002	3.0	3.8	S
1986.8865.....	0.099	26.4	−0.1	0.218	0.004	16.1	3.8	S
1987.2744.....	0.119	25.6	−0.2	0.248	0.000	20.7	3.8	S
1988.1703.....	0.168	23.9	−0.7	0.305	−0.003	42.2	3.6	S
1988.2545.....	0.172	24.7	0.2	0.316	0.003	27.7	3.8	S
1988.9097.....	0.207	23.7	−0.2	0.346	0.002	8.1	1.8	S
1989.01	0.213	25.0	1.2	0.30	−0.05	0.3	0.6	M
1989.17	0.221	25.8	2.1	0.36	0.01	0.1	0.5	M
1989.2294.....	0.224	23.8	0.1	0.360	0.004	28.1	3.8	S
1989.2375.....	0.225	23.9	0.2	0.361	0.005	28.1	3.8	S
1990.841.....	0.311	20.5	−2.0	0.34	−0.05	0.9	1.5	M
1991.0326.....	0.321	21.0	−1.0	0.408	0.011	0.7	1.0	S
1991.25	0.333	22.3	0.0	0.404	0.005	3.1	0.3	H
1991.7189.....	0.358	21.6	−0.4	0.384	−0.018	14.1	4.0	S
1993.0950.....	0.432	20.9	−0.2	0.400	0.002	28.2	4.0	S
1993.7601.....	0.467	19.0	−2.0	0.400	0.010	0.6	1.0	S
1993.8392.....	0.472	21.2	0.6	0.382	−0.007	0.6	1.0	S
1994.8993.....	0.529	19.0	−1.0	0.385	0.017	5.1	1.0	S
1995.1405.....	0.541	20.2	0.5	0.363	0.001	17.9	2.5	S
1995.9186.....	0.583	18.3	−0.7	0.336	−0.004	15.2	2.5	S
1996.8717.....	0.634	18.0	−0.1	0.304	−0.002	12.3	2.5	S
1997.1311.....	0.648	17.2	−0.6	0.293	−0.002	11.4	2.5	S
1997.2323.....	0.654	13.3	−4.4	0.323	0.032	9.9[b]	3.5	S
1997.8273.....	0.686	17.3	0.4	0.257	−0.008	6.6	3.5	S
1997.8301.....	0.686	16.6	−0.3	0.261	−0.004	6.9	3.5	S
1997.8301.....	0.686	16.5	−0.4	0.262	−0.003	6.9	3.5	S
2001.0197.....	0.857	1.2	−1.2	0.073	−0.005	5.0	3.8	S[c]

[a] (M) visual micrometry, (E) eyepiece interferometry, (S) speckle interferometry, and (H) *Hipparcos*.
[b] 3 σ residual in θ and/or ρ; observation was not used in orbital solution.
[c] Previously unpublished observation.

ρ in arcseconds. For each observation, the assigned weight, telescope aperture, and observing technique are also given.

Some measurements made with speckle interferometry were published with position angles differing by 180° from the values tabulated here. This was an inevitable by-product of the quadrant ambiguity inherent in early vector autocorrelation reduction techniques. For most systems, this ambiguity is of little consequence, since the "correct" quadrant usually becomes obvious through orbital analysis or comparison with visual data. When appropriate, some of the quadrants in Table 5 have been adjusted to match, as closely as possible, the values predicted by the new orbit.

4. ORBITAL SOLUTIONS

Differential-correction programs to determine the spectroscopic, visual, and three-dimensional (simultaneous spectroscopic visual) orbits for binary or triple systems, based on the method of nonlinear least squares, have been developed at the University of Victoria (by D. J. B.) and are described in the study of HD 202908 (Fekel et al. 1997). Individual solutions for data of each kind yield standard errors of an observation of unit weight, σ_V, σ_θ, and σ_ρ, for the radial velocities, position angles, and separations, respectively. These are then used as input into solutions for data of more than one dimension, which yield new values for the σ's; these should not differ significantly from the input values if the data are mutually compatible. These programs have been used in other studies such as HR 6469 (Scarfe et al. 1994) and, more recently, 64 Ori (Scarfe, Barlow, & Fekel 2000); they have been used to obtain several solutions for the orbital elements of μ Ori, which are described in the next few paragraphs.

To begin with, the radial velocity data for Aa set out in Tables 2 and 3 were used to obtain a triple-system solution for that subsystem, which gave a standard error of unit weight $\sigma_V = 0.28$ km s^{-1}. Preliminary solutions determined relative weights (DAO 2.4 Å mm^{-1} : DAO 6.5 Å mm^{-1} : McDonald : KPNO = 1.0 : 0.5 : 0.1 : 0.3) that led to similar standard errors of unit weight for each set of observations and showed by the application of Bassett's (1978) second test (Lucy 1989) that the small eccentricity of the short-period orbit is statistically significant. As for 64 Ori (Scarfe et al. 2000), no significant improvement of the precision of the periods was obtained by including observations other than our own. This is due to the low weights that were assigned to the older observations together with their zero-point uncertainties (gains normally expected to be achieved by their inclusion were lost when the systematic differences between observatories were included as additional parameters to be found simultaneously with the orbital elements).

In the next step, the visual and interferometric data set out in Table 5 were used to obtain a visual binary solution. We adopted the weighting system described by Hartkopf, Mason, & Worley (2001a), which is based on observing technique, telescope aperture, binary star separation, and observer expertise.

Initially, separate solutions were obtained from the position angles and separations, and these gave standard errors of unit weight $\sigma_\theta = 1\overset{\circ}{.}8$ and $\sigma_\rho = 0\overset{''}{.}0024$. They were followed by a two-dimensional solution from both quantities simultaneously, in which σ_θ and σ_ρ each increased by only one digit in the second significant figure, an indication of the excellent agreement between the elements in common from the separate solutions.

The differences between the values of the long-period elements common to both the spectroscopic triple-system solution for Aa and the visual binary one, which were obtained from those solutions, were all less than twice their respective uncertainties. Therefore, with $\sigma_V = 0.28$ km s^{-1}, $\sigma_\theta = 1\overset{\circ}{.}8$, and $\sigma_\rho = 0\overset{''}{.}0024$, the two kinds of data were then combined in a simultaneous three-dimensional solution. The value of σ_V remained unchanged to two significant figures and, as in the case of the visual binary solution, σ_θ and σ_ρ each increased by only one digit in the second significant figure, an indication that the elements accurately represent all the data.

Finally, the velocities of Ba and Bb from Table 4 were combined in a triple-system solution for the short-period elements and the amplitude of the long-period variation of the velocity of this close pair's center of mass, with all the other elements of the long-period orbit adopted from the three-dimensional solution. As had been done for the Aa data, preliminary solutions were used to obtain relative weights (for Ba, McDonald : KPNO Fairchild and RCA CCDs : KPNO TI CCD = 0.05 : 0.01 : 0.10, with those for Bb a factor 0.6 smaller still for each data set) that yield the same standard error for an observation of unit weight as the Aa data and showed by the application of Bassett's (1978) second test (Lucy 1989) that the eccentricity of this short-period orbit is without statistical significance. As for HR 6469 (Scarfe et al. 1994), the resulting relative weights for the components of the secondary star are much smaller than those for the primary. Thus, it was not considered worthwhile to obtain a simultaneous solution for all three stars because the long-period elements, except of course for the velocity amplitude of the secondary star, would have been determined almost as they are in our method, solely by the primary.

The elements from the three-dimensional solution for A and the triple-system solution for B are presented in Table 6 and yield the light-time corrections (to the center of mass of the quadruple system) and velocity residuals in Tables 2, 3, and 4 and the visual and interferometric residuals in Table 5, respectively. In Table 6 for the short-period orbital elements of component A, we have chosen to list T_0 rather than T because the eccentricity is so small that the former element is a much more accurate marker than the latter. We also note that the convention for listing the orbital element ω differs for spectroscopic and visual orbits. For the short-period binary component of A, we have listed the value of ω corresponding to the primary, component Aa. For the long-period orbit, which includes both spectroscopic and visual observations, we give the value for component B.

Figure 1 presents the short-period velocity curve for component Aa, where each plotted velocity consists of the observed velocity minus its calculated long-period velocity. Zero phase is a time of maximum positive velocity. Similar short-period velocity curves for components Ba and Bb are shown in Figure 2. Figure 3 presents the velocity curves for the long-period orbit. Zero phase is a time of periastron passage. Each plotted velocity for component A consists of the observed velocity of Aa minus its calculated short-period velocity. For component B, the ratio of the short-period amplitudes,

$$q = K_{\rm Ba}/K_{\rm Bb} = 0.9768 \pm 0.0020\,, \qquad (1)$$

can be used to provide an estimate of the short-period systemic velocity for each pair of velocities, $V_{\rm Ba}$ and $V_{\rm Bb}$, by means of the expression

$$\gamma_B = V_{\rm Ba} + q(V_{\rm Bb} - V_{\rm Ba})/(1+q)\,. \qquad (2)$$

Values of γ_B calculated this way are plotted in Figure 3. Figure 4 shows the ellipse that represents the long-period elements, fitted to the visual and interferometric data.

As a matter of interest, we obtained an additional spectroscopic solution for each subsystem that did not make use of light-time corrections. In each case, a standard variance ratio test indicated that their use had led to a reduction of the sum of the weighted squares of the velocity residuals

TABLE 6
Orbital Elements

Parameter	Short-Period Component A	Short-Period Component B	Long-Period
P (days).....	4.4475858 ± 0.0000012	4.7835361 ± 0.0000028	6809.9 ± 3.4
P (yr).....	...	...	18.644 ± 0.009
T_0 (HJD).....	2,443,740.8761 ± 0.0011[a]	2,443,748.8003 ± 0.0024	...
T (HJD).....	...	...	2,446,083.7 ± 2.2
T (yr).....	...	...	1985.047 ± 0.006
γ (km s^{-1}).....	...	...	42.54 ± 0.03
K_1 (km s^{-1}).....	29.51 ± 0.04	81.78 ± 0.10	14.23 ± 0.07
K_2 (km s^{-1}).....	...	83.72 ± 0.14	15.81 ± 0.16
e.....	0.0044 ± 0.0014	0 (adopted)	0.7426 ± 0.0020
ω (deg).....	289 ± 19[b]	Undefined	215.46 ± 0.30[c]
Ω (deg).....	...	...	24.67 ± 0.14
i (deg).....	...	...	96.20 ± 0.18
a (arcsec).....	...	...	0.2669 ± 0.0014
$a_1 \sin i$ (Gm).....	1.8048 ± 0.0026	5.380 ± 0.007	893 ± 5
$a_2 \sin i$ (Gm).....	...	5.507 ± 0.009	992 ± 11
$M_1 \sin^3 i$ ($M_\odot$)...	...	1.14 ± 0.04	3.03 ± 0.07
$M_2 \sin^3 i$ ($M_\odot$)...	...	1.11 ± 0.03	2.73 ± 0.05
$f(M)$ ($M_\odot$).....	0.01187 ± 0.00004	...	...

[a] See § 4.
[b] Value for component Aa.
[c] Value for component B.

that was significant at the 1% level (the reductions being 64% for the primary and 49% for the secondary). This is more significant than that obtained for HD 202908 (Fekel et al. 1997), where the reduction of 19% was significant at the 5% level but not at the 1% level.

The recent visual orbit of Söderhjelm (1999) has been given a grade of "good" in the Fifth Catalog of Orbits of Visual Binary Stars (Hartkopf et al. 2001a). The elements of Söderhjelm's (1999) orbit are generally in excellent agreement with our new determination. While he did not give errors for the elements, Söderhjelm did note that the number of places to the right of the decimal point for P and a reflects the uncertainties of those elements. This indicates that the uncertainties of our elements are at least a factor of 10 smaller.

5. MAGNITUDE DIFFERENCES

The determination of accurate magnitude differences between components of close visual double stars has long been difficult. The more classical techniques of double-image photometry, wedge photometry, area scanning, double-image micrometry, or even photography are typically much better suited to systems that are more widely separated than the system discussed here. Furthermore, while historically many double star observers have published magnitudes, there is often no differentiation between publishing a magnitude estimate made by the observer and a catalog magnitude published simply to aid in identification. However, some double star observers have published

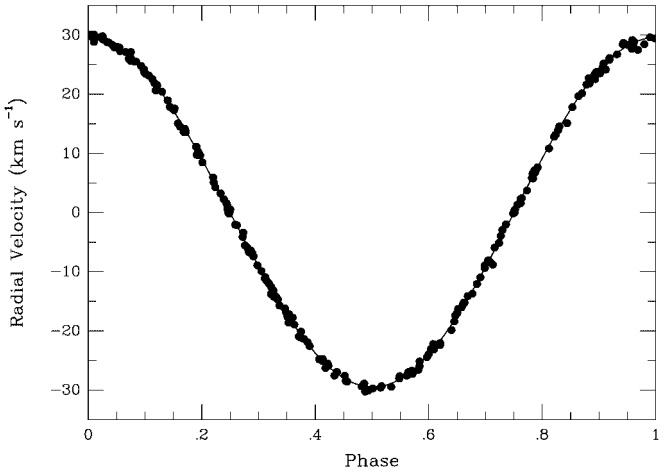

Fig. 1.—Radial velocity curve of μ Ori Aa in its short-period orbit. The points represent the velocities from Tables 2 and 3, minus the velocities of the center of mass of Aa and Ab in the long-period orbit, calculated from the elements in Table 6. The curve represents the short-period elements from the same table. Zero phase is a time of maximum velocity.

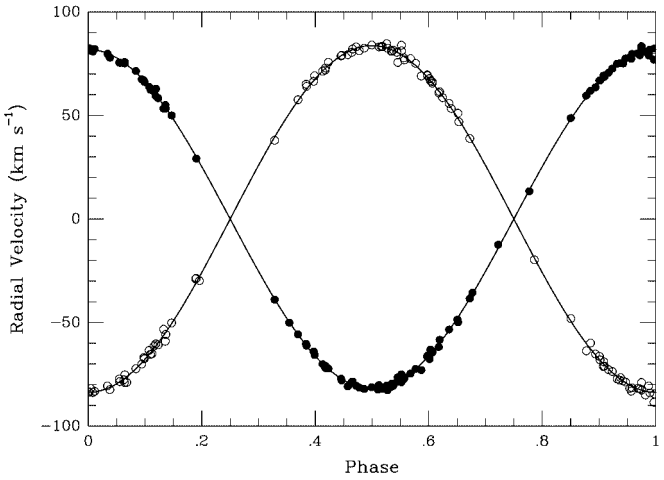

Fig. 2.—Same as Fig. 1, but for μ Ori Ba and Bb. The solid and open symbols represent, respectively, the velocities of Ba and Bb from Table 4, minus the velocities of the center of mass of Ba and Bb in the long-period orbit, calculated from the elements in Table 6. The curves represent the short-period elements from the same table. Zero phase is a time of maximum velocity for Ba.

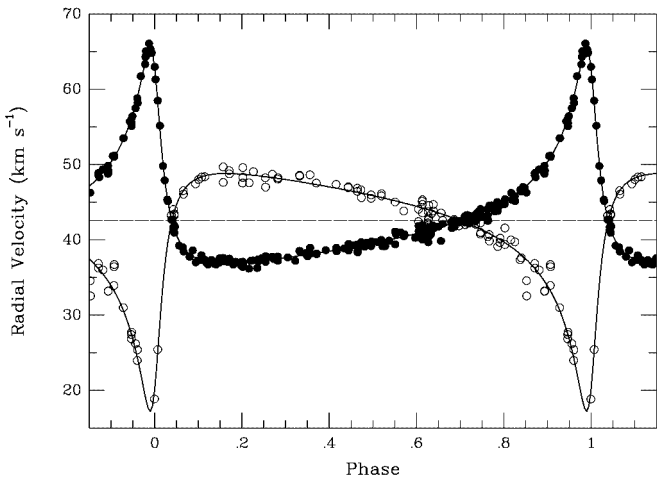

FIG. 3.—Long-period radial velocity curves of μ Ori. The solid symbols represent the velocities of Aa from Tables 2 and 3, minus the velocities in the short-period orbit, calculated from the elements in Table 6. The open symbols represent the velocities of the center of mass of Ba and Bb, calculated by means of equation (2) from the velocities listed in Table 4 for all dates when velocities of both components of B were measured. Dates on which the velocity of only one of those components could be measured are excluded. Zero phase is a time of periastron passage. The curves represent the long-period elements from Table 6.

instead the magnitude difference, the measured or estimated Δm in the observed passband, of the components. In addition some publications (compiled in the USNO Photometric Magnitude Difference Catalog [Worley, Mason, & Wycoff 2001], also known as the Δm Catalog) are specifically tailored for the determination of magnitude differences.

Table 7 contains magnitude difference estimates that were included with the measurements tabulated in the WDS, as well as measurements from the Δm Catalog. Column (1) is the magnitude difference (with error when known). Column (2) contains information regarding the wavelength of observation (effective wavelength and full width at half-maximum [FWHM]). "Broadband visual" indicates a visual estimate made without a filter. With the exception of Baize's (1957) estimate, the determinations are reasonably consistent. The measurement of Labeyrie et al. (1974) was made from a determination of the relative intensities in an autocorrelation map; the authors did not give the FWHM of the filter that was used. The *Hipparcos* filter information is based on Table 1.3.1 of Volume 1 of the *Hipparcos* and Tycho Catalogues (ESA 1997). Column (3) lists the method used, while column (4) gives the reference.

Recently, from observations obtained with the Tycho instrument of *Hipparcos*, Fabricius & Makarov (2000) determined B_T and V_T magnitudes for the visual components of μ Ori. We have converted those Tycho magnitudes to the Johnson system with the formulae in Volume 1 of the *Hipparcos* and Tycho Catalogues (ESA 1997). For the A component, $V = 4.33$ mag and $(B-V) = 0.12$ mag, while the corresponding values for the B component are 6.18 mag and 0.59 mag, respectively. Thus, $\Delta V = 1.85$ mag, which we assume in our calculations.

6. SPECTRAL TYPES

Slettebak (1954) classified component Aa as an Am star with an A3 Ca II K line and an A7 metallic-line spectrum. More recently, Abt & Morrell (1995) determined the spectral classes of its Ca II K, Balmer, and metallic lines to be A4, A5, and A7, respectively.

We planned to determine the spectral types of μ Ori with a spectrum addition technique used by Strassmeier & Fekel (1990). They identified several luminosity-sensitive and temperature-sensitive line ratios in the 6430–6455 Å region and used them, along with the general appearance of the spectrum, as spectral type criteria for F, G, and K stars. From the list of Abt & Morrell (1995), the spectra of 10 slowly rotating Am stars with classifications similar to those of μ Ori were obtained at KPNO with the same telescope, spectrograph, and detector as our spectra of μ Ori. The spectra of various F stars from the list of Keenan & McNeil (1989) were obtained similarly. The wavelength region around 6430 Å contains primarily Fe I lines but also has three Fe II features and three Ca I lines. Unfortunately, we were unable to find a satisfactory Am-type reference star to compare with μ Ori Aa. Most of the observed Am stars were rotating more rapidly than μ Ori Aa and often had weaker Fe I lines, while in one star, HR 4750, lines of a secondary component were found.

Canonical relations, such as those of Gray (1992), for spectral class versus mass, spectral class versus color, and spectral class versus absolute magnitude can be used to get an initial estimate of the spectral types of Ba and Bb. The nearly identical masses of 1.4 $M_\odot$, determined in § 8, indicate a mid F spectral type for each component. On the other hand, $(B-V) = 0.59$, derived for the B visual component from the Tycho photometry, as well as the V-magnitude difference for the A-B system, imply a late F spectral class for the mean component of B. Although these estimates differ somewhat, they indicate that components Ba and Bb are approximately a full spectral class later than Aa.

In an attempt to improve the estimate of their spectral types, comparison spectra were created with a computer program developed by Huenemoerder & Barden (1984) and Barden (1985). Various combinations of F-type reference-star spectra were rotationally broadened, shifted in radial velocity, appropriately weighted, and added together with a featureless continuum representing Aa. Those combination spectra were compared with the observed spectrum of μ Ori. Estimation of the spectral types is made more difficult because, as shown in Fig. 1 of Fekel (1980), the lines of Ba and Bb are quite weak, having residual intensities of only 2%–3%. While the rotational velocities of the two stars differ, the spectral types of Ba and Bb appear to be very similar, and identical spectral types were assumed. The best combination spectrum is between mid and late F stars. The Fe I blend at 6400 Å is fitted a bit better by stars of late F type, but the three Fe II lines are fitted better by mid F stars. Thus, we estimate a spectral type of F5: V for both Ba and Bb with a magnitude difference of 0.0. The colon indicates that the classifications are more uncertain than usual because of the difficulties discussed above.

As noted earlier, the V magnitude difference between components A and B is nearly 2 mag. Thus, Ba and Bb are quite faint relative to Aa, and, of course, we are unable to detect the spectrum of Ab at all, although presumably it is a main-sequence star even cooler and fainter than Bb. Since the light of the Am-type star dominates the system, it is not surprising that the $U-V$, $V-R$, and $V-I$ color indices of μ Ori published by Johnson et al. (1966) are quite similar to those of other stars of the same $B-V$ and of mid-to-late A

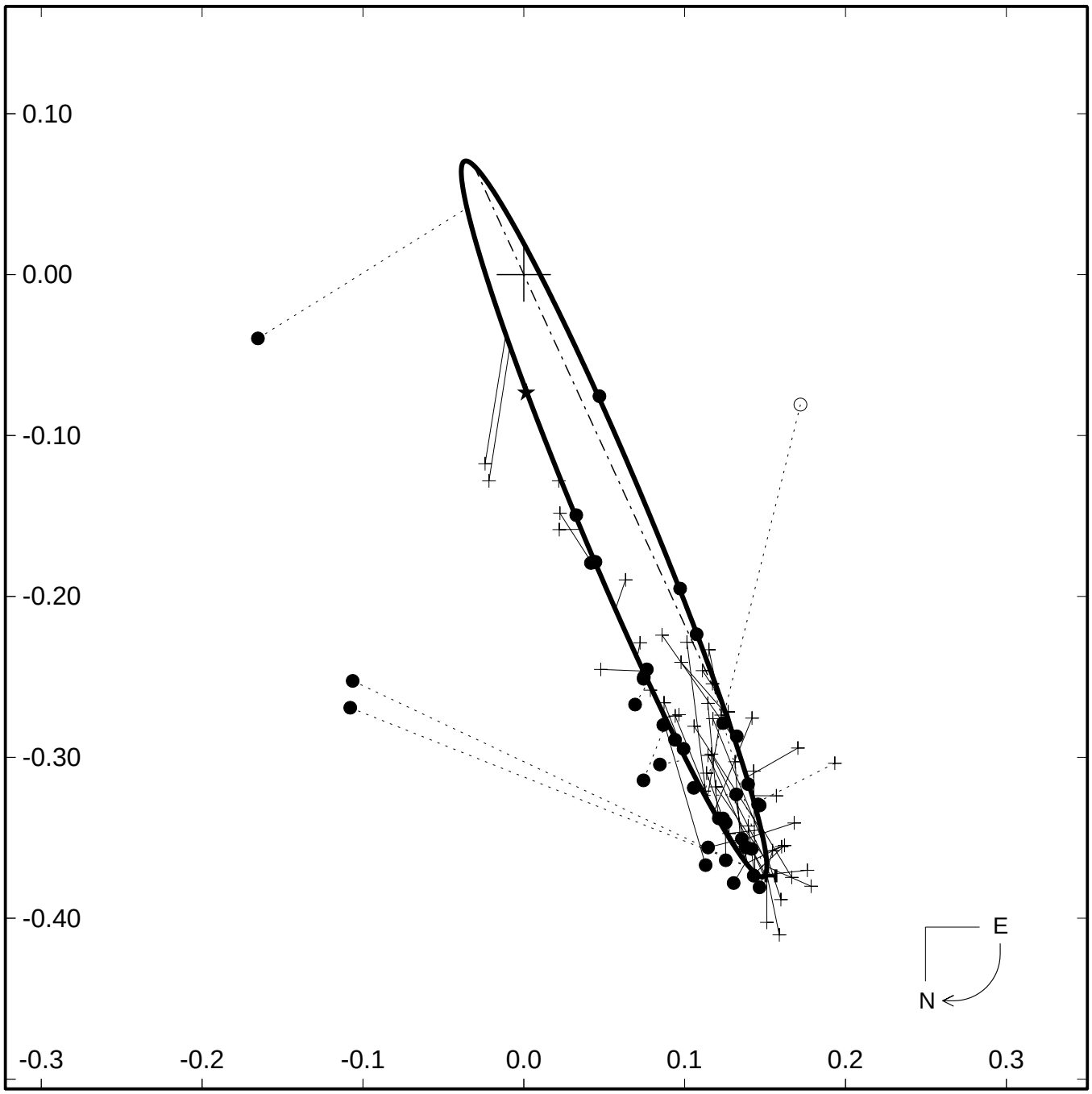

FIG. 4.—Relative visual orbit for μ Ori = A2715 AB. The large plus sign marks the position of component A, and the calculated orbit for B is shown as a heavy ellipse; the dot-dashed line indicates the line of nodes. Measurements made by visual micrometry, eyepiece interferometry, and speckle interferometry are indicated by plus signs, open circles, and filled circles, respectively. The previously unpublished speckle measurement of 2001 is represented as a filled star. Observations are connected by solid lines to their predicted positions on the ellipse. Those given zero weight in the final orbital solution are connected to the ellipse by dotted lines. Scales are in arcseconds.

type. Nevertheless, we combined the colors from Johnson (1966) for stars with mid A and mid-to-late F spectral types in an attempt to reproduce the color indices of the composite μ Ori system (Johnson et al. 1966). For the visual components, the V mag difference of 1.85, computed from the Tycho photometry, was adopted. As expected, the colors do not provide as strong a determination of the spectral types of the F stars as one might like. In agreement with the spectroscopy, a combination of an A5 V star and a pair of F5 V stars (Table 8) produces slightly better results than an A5 V plus two F8 V components.

7. PROJECTED ROTATIONAL VELOCITIES

Like many metallic-line stars, component Aa is slowly rotating. Slettebak (1954) found a $v \sin i$ of 20 km s^{-1}, while

TABLE 7
MAGNITUDE DIFFERENCES

Δm (mag) (1)	Wavelength (Å) (2)	Method (3)	Reference (4)
1.6	Broadband visual	Objective grating	1
2.6	Broadband visual	Micrometer	2
1.6	Broadband visual	Micrometer	3
1.7	Broadband visual	Micrometer	4
1.5	Broadband visual	Micrometer	4
1.1	Broadband visual	Micrometer	5
1	5450	Speckle autocorrelation relative intensity	6
1.75 ± 0.06	7980 ± 1080	Adaptive optics	7
1.31 ± 0.02	8840 ± 1220	Adaptive optics	7
1.95 ± 0.02	$\sim 5000 \pm 2200$ (H_p)	*Hipparcos*	8
1.90 ± 0.01	5050 ± 970 (T_V)	Tycho	9
2.34 ± 0.01	4350 ± 700 (T_B)	Tycho	9

REFERENCES.—(1) Kuiper 1950; (2) Baize 1957; (3) Kuiper 1961; (4) Worley 1962; (5) Worley 1972; (6) Labeyrie et al. 1974; (7) ten Brummelaar et al. 1996; (8) ESA 1997; (9) Fabricius & Makarov 2000.

Abt & Morrell (1995) estimated 18 km s^{-1}. Recently, Debernardi et al. (2000) measured a much smaller value of 10.6 km s^{-1} from CORAVEL observations.

We have determined projected rotational velocities of the components with the procedure of Fekel (1997). For each component, the FWHM was measured for several metal lines in the 6430 Å region, and the results were averaged. An instrumental broadening of 0.21 Å was found by taking the square root of the difference between the squares of measurements of the stellar and comparison lines and was removed from the measured broadening, yielding the intrinsic broadening. A calibration polynomial was used to convert this broadening in angstroms into a total line broadening in kilometers per second. For the Am star, this broadening was assumed to be the rotational velocity, while for the two mid F stars, a macroturbulence of 4 km s^{-1} was assumed and removed.

From an average of 14 spectra, component Aa has $v \sin i = 9.7$ km s^{-1} with an estimated uncertainty of 1.0 km s^{-1}. Our value is in excellent agreement with the CORAVEL measurements. Although the strongest lines of Ba and Bb have depths of only 2%–3% in the 6430 Å region, it is obvious from visual inspection of those spectra that the two components have rather different projected rotational velocities. The $v \sin i$ values for Ba and Bb are 6.5 ± 2.0 and 11.2 ± 2.0 km s^{-1}, respectively, both of which are means from 11 spectra. We caution, however, that because the lines of Ba and Bb are quite weak, noise and possible blends from other lines may cause our measured $v \sin i$ values of these two components to be systematically too large.

TABLE 8
MAGNITUDES OF THE COMPONENTS OF μ ORI

Component	Spectral Type	U (mag)	B (mag)	V (mag)	R (mag)	I (mag)
Aa	A5 V	4.56	4.45	4.31	4.15	4.09
Ba	F5 V	7.34	7.34	6.91	6.50	6.27
Bb	F5 V	7.34	7.34	6.91	6.50	6.27
Combined	...	4.40	4.31	4.13	3.93	3.83
Observed	...	4.40	4.29	4.13	3.94	3.86

8. DYNAMICAL PARAMETERS

Our orbital solutions provide directly the masses of Ba and Bb and the total mass of the system Aa plus Ab, as well as the mass function of that system, $f_A(M)$. From them, it is also easy to deduce the orbital parallax, distance, and distance modulus of the system. All these quantities are presented in the first part of Table 9, except for $f_A(M)$, which is the last entry in Table 6. The inclination of the short-period orbit of component B is also readily found from the other elements of that orbit as is the total mass of B derived from

TABLE 9
DYNAMICAL PARAMETERS

Parameter	Value
M_A ($M_\odot$)	3.076 ± 0.071
M_B ($M_\odot$)	2.770 ± 0.049
$M_{\rm Ba}$ ($M_\odot$)	1.401 ± 0.028
$M_{\rm Bb}$ ($M_\odot$)	1.369 ± 0.028
Orbital parallax (arcsec)	0.02107 ± 0.00018
Distance (pc)	47.46 ± 0.40
Distance modulus	3.381 ± 0.18
i_B (deg)	68.84 ± 0.88
M_V(Aa) (mag)	0.93 ± 0.04
M_V(Ba) (mag)	3.53 ± 0.15
M_V(Bb) (mag)	3.53 ± 0.15
$L_{\rm Aa}$ ($L_\odot$)	32.2 ± 1.5
$L_{\rm Ba}$ ($L_\odot$)	3.0 ± 0.4
$L_{\rm Bb}$ ($L_\odot$)	3.0 ± 0.4
$R_{\rm Aa}$ ($R_\odot$)	2.85 ± 0.19
$R_{\rm Ba}$ ($R_\odot$)	1.33 ± 0.11
$R_{\rm Bb}$ ($R_\odot$)	1.33 ± 0.11
Angular momenta:	
J_L ($M_\odot$ AU^2 yr^{-1})	52.83 ± 1.84
J_B ($M_\odot$ AU^2 yr^{-1})	2.025 ± 0.061
Direction of $\boldsymbol{J}_L$:	
Equatorial coordinates (J2000.0):	
A	$11^{\rm h}18^{\rm m}14^{\rm s} \pm 48^{\rm s}$
D	$-23^\circ 5' 4 \pm 8'.4$
Galactic coordinates:	
L	$276^\circ.57 \pm 0^\circ.21$
B	$34^\circ.96 \pm 0^\circ.15$

the long-period orbit; both of which are presented in Table 9.

Next, it is not difficult to show that if i_A is the unknown inclination of the plane of the mutual orbit of Aa and Ab, then

$$M_{\rm Ab} \sin i_A = [f_A(M) M_A^2]^{1/3} . \quad (3)$$

Since both quantities on the right side of this equation are known accurately, it yields

$$M_{\rm Ab} \sin i_A = 0.4821 \pm 0.0075 \quad (4)$$

in solar units. This constrains quite tightly, for any choice of i_A, the values of both $M_{\rm Ab}$ and $M_{\rm Aa}$, since the sum of the latter two is known. Masses in Figure 5, $M_{\rm Aa}$ and $M_{\rm Ab}$ are plotted as functions of i_A.

It is clear that $M_{\rm Ab}$ cannot be smaller than 0.48 $M_\odot$ for any real value of i_A and hence that $M_{\rm Aa}$ cannot be larger than 2.60 $M_\odot$. Assuming Ab to be a main-sequence star and not a degenerate one, the opposite extreme is provided by the fact that Ab is invisible in the spectrum. It is hardly likely to have a mass greater than about 1.2 $M_\odot$, which is scarcely 0.2 $M_\odot$ less than those of Bb and Ba. Thus, the mass of Aa must be at least 1.85 $M_\odot$ and i_A at least 23°. From its spectral type, the mass of Aa might be expected to be near the low end of the above range, i.e., about 1.8–2.0 $M_\odot$. However, the magnitude difference of 2.6 between Aa and Ba, interpreted as a bolometric one, suggests a mass near the top of the range, if we adopt the mass-luminosity relationship $L = M^4$ in solar units.

We used our orbital parallax plus the apparent visual magnitudes of the individual components listed in Table 8 to determine the absolute visual magnitudes of 0.93, 3.53, 3.53 mag for Aa, Ba, and Bb, respectively. Because the system is less than 50 pc away, we did not include any interstellar reddening. We then computed the luminosities and radii of the components. For spectral types A5 V and F5 V, we adopted the colors of Johnson (1966) and used the corresponding bolometric corrections, which are quite small, and effective temperatures from Flower (1996). All these derived fundamental quantities are listed in Table 9.

Turning now to the orbital angular momenta, it is easy to derive that of the long-period orbit, $\boldsymbol{J}_L$, as a vector, as well as the magnitude, J_B, of that of the short-period orbit of component B. These quantities are included in Table 9. As expected, the magnitude of $\boldsymbol{J}_L$ is more than an order of magnitude larger than J_B. For the short-period orbit of A, the angular momentum J_A cannot be found, since the individual stellar masses are unknown, but it can be expressed in terms of the product $M_{\rm Aa} M_{\rm Ab}$ as

$$J_A = 2.011 \times 10^{-12} K_{\rm Aa}^5 P_A^2 (1 - e_A^2)^3 f_A(M)^{-5/3} M_A^{-1/3} \times (M_{\rm Aa} M_{\rm Ab}) . \quad (5)$$

Here M_A comes from the long-period orbit and everything else from the short-period orbit of Aa. This equation can be simplified by substituting for $f_A(M)$,

$$f_A(M) = 1.0361 \times 10^{-7} K_{\rm Aa}^3 P_A (1 - e_A^2)^{3/2} , \quad (6)$$

to obtain

$$J_A = 0.8798 P_A^{1/3} M_A^{-1/3} (1 - e_A^2)^{1/2} (M_{\rm Aa} M_{\rm Ab}) , \quad (7)$$

which, in turn, yields

$$J_A = (0.9948 \pm 0.0077)(M_{\rm Aa} M_{\rm Ab}) . \quad (8)$$

The maximum possible value of J_A is 2.35 $M_\odot$ AU^2 yr^{-1}, for $M_{\rm Aa} = M_{\rm Ab}$, but for more likely values of those masses, J_A will probably be slightly less than J_B. Thus, even though the orbits cannot be coplanar, the direction of the total angular momentum must be closely similar to that of $\boldsymbol{J}_L$.

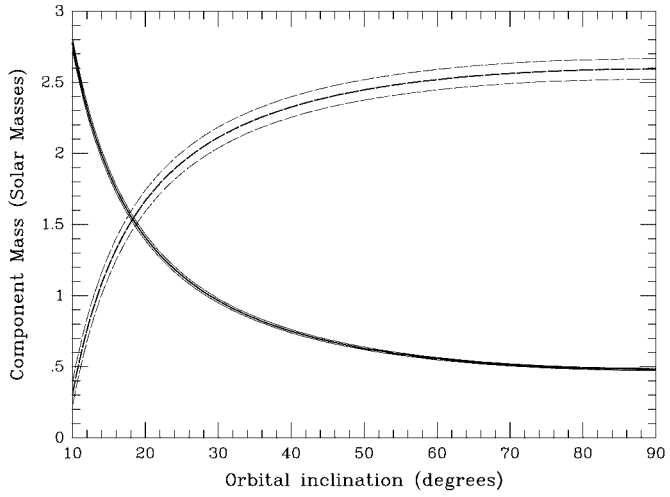

FIG. 5.—Masses of μ Ori Aa (*dashed curves*) and Ab (*solid curves*) plotted against the inclination of their mutual orbit. In each group of three curves, the central one assumes the most probable values of the short-period orbit's mass function and the combined mass. The upper and lower curves assume values larger and smaller by 1 σ, respectively; at the scale of this figure, the curves for Ab are not resolved and appear as a single thick curve. The uncertainty of $M_{\rm Aa}$ is larger than that of $M_{\rm Ab}$ at any inclination because it depends more strongly on the relatively poorly determined total mass of the pair.

9. DISCUSSION

Our computed absolute visual magnitudes for the Ba and Bb components (Table 9) are exactly those expected for two F5 V stars, according to the canonical relations of Gray (1992). However, for component Aa, our absolute visual magnitude is over 1 mag brighter than expected. Burkhart & Coupry (1989) included μ Ori in an abundance analysis of Am-type stars in the Hyades cluster. For Aa, the Am component, they estimated an iron abundance that is slightly greater than solar but somewhat less than the iron abundance of several Am stars in the Hyades.

As a result, we have compared the components of μ Ori with the $Z = 0.02$ evolutionary tracks of Schaller et al. (1992). Figure 6 shows four evolutionary tracks with masses ranging from 1.25 to 2.5 $M_\odot$ and the positions of the three visible components. In the figure, the positions of Ba and Bb are identical, since we have adopted a magnitude difference of 0.0. As noted previously, effective temperatures for the stars are from the scale of Flower (1996). The uncertainties in the temperatures are estimated to be 250 K for Aa and 200 K for Ba and Bb. The temperature uncertainty for Aa is based on differences in the temperature scales of Gray (1992) and Flower (1996). The temperature uncertainty of Ba and Bb results from considerations of spectral type uncertainties, uncertainty in the magnitude difference between Ba and Bb, and temperature calibration differ-

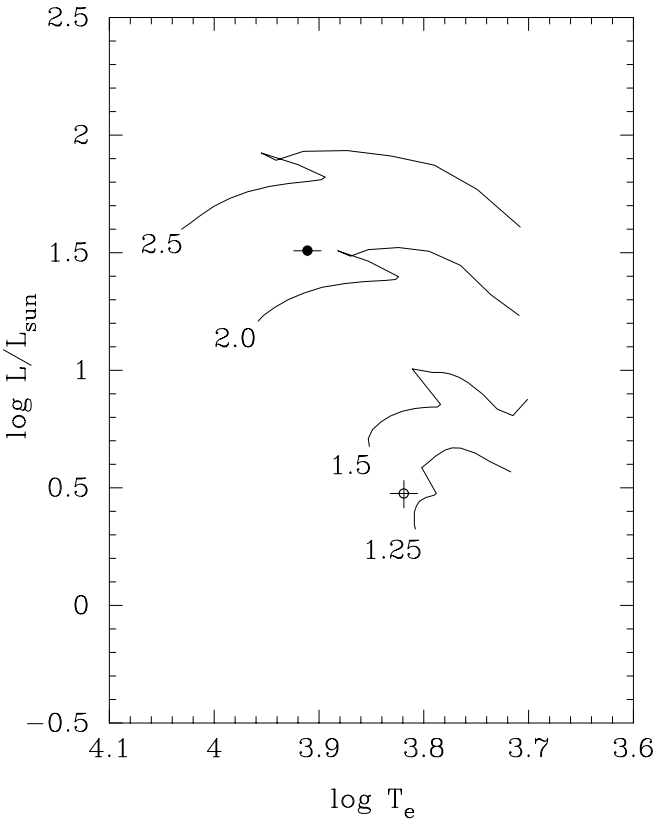

FIG. 6.—Components of μ Ori compared with four evolutionary tracks, all with $Z = 0.02$ but for different masses (labeled in units of solar mass), from Schaller et al. (1992). Component Aa is the filled circle. The error bars for its luminosity uncertainty are covered by the symbol. Components Ba and Bb are represented by the open circle.

ences. For Aa, the luminosity uncertainty is smaller than the plotted symbol, while the increased uncertainty for Ba and Bb results from the inclusion of uncertainty for their magnitude difference.

The position of Aa is consistent with an A-type star having a mass of 2–2.2 $M_\odot$, which, compared with the total mass of component A, suggests that Ab, the unseen component, is probably a G or early K dwarf. The evolutionary tracks indicate that Aa has an age of 1 billion yr and is near the end of its main-sequence lifetime. The Ba and Bb components are close to the zero-age main sequence with masses of 1.3–1.35 $M_\odot$, reasonably consistent with their F5: V spectral types and our computed masses of 1.4 $M_\odot$.

Tidal effects (see, e.g., Zahn 1977) and/or a hydrodynamic mechanism (Tassoul 1987) can produce rotational synchronization in binary components and circularization of their orbit. The masses of components Ba and Bb indicate that the spectral types and radii of the two stars should be quite similar. Our computed radius of 1.33 $R_\odot$ (Table 9) for each of those two components is essentially identical with canonical values. Thus, we adopted our radius to compute a synchronous rotation velocity of 14.1 km s^{-1} for both components. Using the orbital inclination of the Ba-Bb system (Table 9) and assuming, as is usually done, that the rotation and orbital axes are parallel, we computed $v \sin i = 13.1$ km s^{-1}. Our measured $v \sin i$ values are 6.5 ± 2.0 and 11.1 ± 2.0 km s^{-1} for Ba and Bb, respectively. It is clear, therefore, that Ba is far from synchronously rotating, unless the assumption of parallel axes is incorrect. Component Bb is rotating more rapidly and, within the uncertainties, may be synchronously rotating.

For component Aa, the Am star, a radius of 2.85 $R_\odot$ and orbital period of 4.448 days result in a synchronous rotation velocity of 32.4 km s^{-1}. Combining our $v \sin i$ with that of Debernardi et al. (2000), we determined a mean of 10.2 km s^{-1}. Thus, if the rotation is synchronous, the inclination of the axis is 18°. If we again assume that the rotation and orbital axes are parallel, the mass of Ab, the unseen component of the quadruple system, would be 1.5 $M_\odot$, nearly 50% of the mass sum for component A. Based on the known properties of Aa, such a low orbital inclination and, therefore, synchronous rotation can be ruled out.

Both tidal theory (Zahn 1977) and the hydrodynamic mechanism of Tassoul (1987) are in agreement that the timescale for rotational synchronization is much shorter than that for orbital circularization. Thus, we might expect both short-period orbits to have at least modest eccentricities, but such is not the case. Components Ba and Bb have a circular orbit, while the orbit for Aa and Ab, with an eccentricity of less than 0.01, is nearly circular. This apparent contradiction with theory, however, may simply result from eccentricities that initially were close to zero.

In triple systems, the third star may cause some of the orbital elements of the close pair to vary with time. Changes in the eccentricity have been examined numerically by Mazeh & Shaham (1979) and both analytically and numerically by Söderhjelm (1984). Their results showed that even if the short-period system attained a circular orbit, its eccentricity would be modulated. From Mazeh & Shaham (1979), we computed a modulation period of 56,000 yr.

Fekel (1981) compared the short- and long-period orbital inclinations for 20 multiple star systems and found that at least 33% of the orbital pairs are not coplanar. For μ Ori, the visual orbit has an inclination of 96°.2. The minimum angle between the plane of that orbit and that of the Ba–Bb orbit is 15°, making them noncoplanar. Although the possibility that the visual and Aa-Ab orbits are coplanar cannot be dismissed, coplanarity requires almost the maximum possible mass for Aa ($\sim$2.6 $M_\odot$) and the minimum for Ab ($\sim$0.5 $M_\odot$). The properties of the Am star compared with evolutionary tracks suggest $27° < i_A < 34°$, and so these two orbits are probably not coplanar.

In the near future, it may be possible to resolve the short-period orbits and determine the inclinations directly. Observed at visual wavelengths, the subsystems of components A and B are just at the limiting resolution of the CHARA Interferometric Array on Mount Wilson.

We thank Daryl Willmarth and Jeannette Barnes of NOAO for their help over the many years. We also thank Murray Fletcher for his skill and care in maintaining the ARCTURUS measuring machine, particularly after it was moved in 1997 from the DAO office building to the optical shop. W. I. H. and B. D. M. wish to thank the US Naval Observatory for their continued support of the double star program. This research has been supported in part by NASA grants NCC 5-551, NCC 5-96, and NSF grant HRD-9706268 to Tennessee State University, and in part by grants from the Natural Sciences and Engineering Research Council (NSERC) of Canada and from the University of Victoria.

REFERENCES

Abt, H. A., & Levy, S. G. 1985, ApJS, 59, 229
Abt, H. A., & Morrell, N. I. 1995, ApJS, 99, 135
Abt, H. A., Sanwal, N. B., & Levy, S. G. 1980, ApJS, 43, 549
Aitken, R. G. 1914, Lick Obs. Bull., 8, 93
Alden, H. L. 1942, AJ, 50, 73
Baize, M. P. 1957, J. Obs., 40, 165
Barden, S. C. 1985, ApJ, 295, 162
Bassett, E. E. 1978, Observatory, 98, 122
Bourgeois, P. 1929, ApJ, 70, 256
Burkhart, C., & Coupry, M. F. 1989, A&A, 220, 197
Debernardi, Y., Mermilliod, J.-C., Carquillat, J.-M., & Ginestet, N. 2000, A&A, 354, 881
ESA. 1997, The Hipparcos and Tycho Catalogues (ESA SP-1200) (Noordwijk: ESA)
Fabricius, C., & Makarov, V. V. 2000, A&A, 356, 141
Fekel, F., Bopp, B. W., & Lacy, C. H. 1978, AJ, 83, 1445
Fekel, F. C. 1980, PASP, 92, 785
———. 1981, ApJ, 246, 879
———. 1992, in ASP Conf. Ser. 32, Complementary Approaches to Double and Multiple Star Research, ed. H. A. McAlister & W. I. Hartkopf (IAU Colloq. 135) (San Francisco: ASP), 89
———. 1997, PASP, 109, 514
———. 1999, in ASP Conf. Ser. 185, Precise Stellar Radial Velocities, ed. J. B. Hearnshaw & C. D. Scarfe (IAU Colloq. 170) (San Francisco: ASP), 378
Fekel, F. C., Scarfe, C. D., Barlow, D. J., Duquennoy, A., McAlister, H. A., Hartkopf, W. I., Mason, B. D., & Tokovinin, A. A. 1997, AJ, 113, 1095
Fitzpatrick, M. J. 1993, in ASP Conf. Ser. 52, Astronomical Data Analysis Software and Systems II, ed. R. J. Hanisch, R. V. J. Brissenden, & J. Barnes (San Francisco: ASP), 472
Flower, P. J. 1996, ApJ, 469, 355
Frost, E. B. 1906, ApJ, 23, 264
Frost, E. B., Barrett, S. B., & Struve, O. 1929, Publ. Yerkes Obs., 7, Part 1, 27
Frost, E. B., & Struve, O. 1924, ApJ, 60, 192
Giclas, H. L., Burnham, R., & Thomas, N. G. 1962, Lowell Obs. Bull., 5, 257
Gray, D. F. 1992, The Observation and Analysis of Stellar Photospheres (Cambridge: Cambridge Univ. Press), 431
Hartkopf, W. I., Mason, B. D., & Worley, C. E. 2001a, AJ, 122, 3472
Hartkopf, W. I., McAlister, H. A., & Mason, B. D. 2001b, AJ, 122, 3480
Heintz, W. D. 1989, PASP, 101, 510
Huenemoerder, D. P., & Barden, S. C. 1984, BAAS, 16, 510
Johnson, H. L. 1966, ARA&A, 4, 193
Johnson, H. L., Mitchell, R. I., Iriarte, B., & Wisniewski, W. Z. 1966, Comm. Lunar Planet. Lab., 4, 99
Keenan, P. C., & McNeil, R. C. 1989, ApJS, 71, 245
Kuiper, G. P. 1950, J. Obs., 33, 1
———. 1961, ApJS, 6, 1
Labeyrie, A., Bonneau, D., Stachnik, R. V., & Gezari, D. Y. 1974, ApJ, 194, L147
Lucy, L. B. 1989, Observatory, 109, 100
Mason, B. D., Wycoff, G. L., Hartkopf, W. I., Douglass, G. G., & Worley, C. E. 2001, AJ, 122, 3466
Mazeh, T., & Shaham, J. 1979, A&A, 77, 145
Osvalds, V. 1964, Publ. McCormick Obs., 11, 175
Perryman, M. A. C., et al. 1998, A&A, 331, 81
Popper, D. M. 1949, ApJ, 109, 100
Richardson, E. H. 1968, JRASC, 62, 313
Scarfe, C. D. 1967, PASP, 79, 414
Scarfe, C. D., Barlow, D. J., & Fekel, F. C. 2000, AJ, 119, 2415
Scarfe, C. D., Barlow, D. J., Fekel, F. C., Rees, R. F., Lyons, R. W., Bolton, C. T., McAlister, H. A., & Hartkopf, W. I. 1994, AJ, 107, 1529
Scarfe, C. D., Batten, A. H., & Fletcher, J. M. 1990, Publ. Dom. Astrophys. Obs., 18, 21
Schaller, G., Schaerer, D., Meynet, G., & Maeder, A. 1992, A&AS, 96, 269
Slettebak, A. 1954, ApJ, 119, 146
Söderhjelm, S. 1984, A&A, 141, 232
———. 1999, A&A, 341, 121
Strassmeier, K. G., & Fekel, F. C. 1990, A&A, 230, 389
Tassoul, J.-L. 1987, ApJ, 322, 856
ten Brummelaar, T. A., Mason, B. D., Bagnuolo, W. G., Hartkopf, W. I., McAlister, H. A., & Turner, N. H. 1996, AJ, 112, 1180
van Bueren, H. G. 1952, Bull. Astron. Inst. Netherlands, 11, 385
Worley, C. E. 1962, AJ, 67, 403
———. 1972, Publ. USNO, 22, Part 4
Worley, C. E., Mason, B. D., & Wycoff, G. L. 2001, AJ, 122, 3482
Zahn, J.-P. 1977, A&A, 57, 383